Journal of Materials Chemistry C

Accepted Manuscript

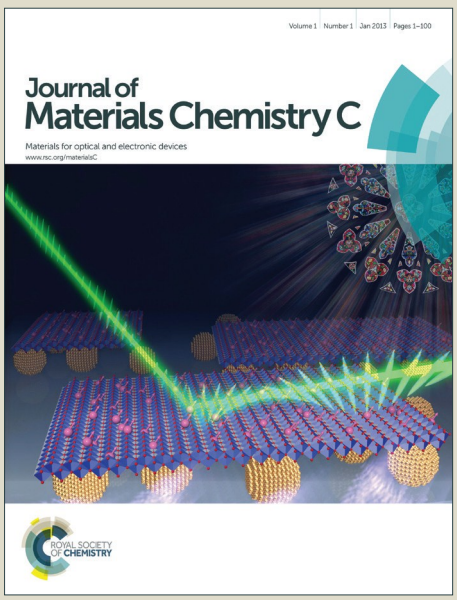

ROYAL SOCIETY OF CHEMISTRY

www.rsc.org/materialsC

A mono(carboxy) porphyrin-triazine-(Bodipy)$_2$ Triad as Donor for Bulk Heterojunction Organic Solar Cells

Ganesh D. Sharma [1] S. A. Siddiqui,[1] Agapi Nikiforou,[2] Galateia E. Zervaki,[2] Irene Georgakaki,[2] Kalliopi Ladomenou,[2] Athanassios G. Coutsolelos[2]**

To the memory of our colleague and friend, John Mikroyannidis

Ganesh D. Sharma, Prof., S. A. Siddiqui,
R&D Centre for Engineering and Science, JEC Group of Colleges, Jaipur Engineering College Campus, Kukas, Jaipur, Raj 303101, India
E-mail: gdsharma273@gmail.com

Athanassios G. Coutsolelos, Prof., Agapi Nikiforou, Galateia E. Zervaki,PhD,Irene Georgakaki, Dr., Kalliopi LadomenouDr.
Department of Chemistry, Laboratory of Bioinorganic Chemistry, University of Crete, Voutes Campus, P.O. Box 2208, 71003, Heraklion, Crete, Greece
E-mail: coutsole@chemistry.uoc.gr

Keywords: Porphyrin, Bodipy, BHJ, Organic solar cells.

Abstract

In the present article bulk heterojunction (BHJ) solution processed organic solar cells have been prepared using mono(carboxy)porphyrin-triazine-(Bodipy)$_2$triad **(PorCOOH)(BDP)$_2$** as a donor and ([6,6]-phenyl C_{71} butyric acid methyl ester) ($PC_{71}BM$) as an acceptor. This donor/acceptor system aims at the of increasing the light capturing process efficiency of the device. The solution processed BHJ organic solar cell with an optimized weight ratio of 1:1 **(PorCOOH)(BDP)$_2$**:$PC_{71}BM$ processed with THF as a solvent showed an overall power conversion efficiency (PCE) of 3.48 % with short circuit current J_{sc}= 8.04 mA/cm^2, open circuit voltage V_{oc}= 0.94 V and fill factor FF =0.46. The relatively high value of V_{oc} was attributed to the deeper highest occupied molecular orbital energy level of **(PorCOOH)(BDP)$_2$**. When the active layer of the solar cell was processed from a mixture of 4% v/v of pyridine in THF solvent, it achieved a PCE value of 5.29 % with J_{sc} =10.48 mA/cm^2, V_{oc} =0.90 V and FF=0.56. This was ascribed to the enhancement of both the J_{sc} and the FF values. The higher value of J_{sc} is explained by the increased absorption profile of the blend, the stronger incident photon to current efficiency (IPCE) response and the higher crystallinity of the active layer, induced by the solvent additive while the enhancement of FF may be due to the better charge transport capability and the charge collection efficiency in the later device.

1. Introduction

Organic solar cells (OSCs) based on a bulk heterojunction (BHJ) active layer that typically consists of a blend of a photoactive polymer or small molecule as electron donor and fullerene derivatives as electron acceptor, have been promising candidates and have attracted much attention due to certain advantages such as solution processability of their active layer, light weight, flexibility and potential low costs.[1-4] With the rapid progress over the last decades, where power conversion efficiencies (PCEs) over 9 %[5-8] for single junction and 11% for tandem junction solar cells[9-11] have been achieved. These are based on BHJ polymer solar cells with a low bandgap conjugated polymer as electron donor and fullerene derivatives as electron acceptor, after the optimization of interface layer and morphology. Recently, Tan et al. reported high-performance single-junction OSCs with an efficiency of 10% by implementing the deterministic aperiodic nanostructures (DAN) patterning for broadband self-enhanced light absorption with optimum charge extraction.[12] However, the polymer used in such a device is still expensive, suffering from difficulties of multi-step synthesis, reproducibility, purification for uniform molecular weight, and high dispersity.

Recently, alternative to organic polymers, small organic molecules have been utilized as photoactive electron donors, owing to their potential advantages in terms of definite molecular structure and molecular weight, high purity and facile synthesis and good batch-to-batch reproducibility.[13-20] Up to date, OSCs based on a small molecule as donor along with $PC_{71}BM$ as electron acceptor have reached efficiencies in the range of 8-10%.[11, 21-25]

Among other small molecules that could function as electron donors in OSCs are porphyrins - the synthetic analogues of chlorophylls - are of special interest, since they are known to model nature's choice aslight harvesting antennae systems that are involved in energy and electron transfer processes in many biological systems. Furthermore, they exhibit large molar absorption coefficients,[26,27] tunable and photophysical properties via central metal modification and/or introduction of suitable substituents at the macrocycle peripheral

positions.[28,29] Despite the successful use of porphyrins as sensitizers in dye-sensitized solar cells (DSSCs)[30-33] (devices with PCE values higher than 12% have been reported), their utilization as donors in solution-processed BHJ organic solar cells is rather limited because of their poor solubility in common organic solvents. However, the appropriate selection of peripheral substituents can increase their solubility. Recent progress in this area of research resulted in solution-processed BHJ solar cells based on suitable porphyrin derivatives as donors, along with $PC_{71}BM$ as electron acceptor,that displayed PCEs from 2.5% to 7.23%, after device optimization.[34-40] Furthermore, an OSC based on a porphyrin based on two dimesional (2D) donor –acceptor (D-A) polymer used as donor, along with $PC_{71}BM$ acceptor, showed a PCE value of 8.0%, without using any additives, which was further improved up to 8.68% when a cathodic interlayer was used to diminish the leakage current.[41]

Despite the strong Soret- and moderate Q band absorptions of porphyrins (in 400-450 and 550-700 nm, respectively), they exhibit poor absorption characteristics 450 and 550 nm. Efforts have been made towards the design and synthesis of π-extended porphyrins which absorb in this wavelength region.[42,43] Boron-dipyrromethane (BDP) belongs to a class of fluorescent dyes that exhibit spectral characteristics in that particular area.[44-46] By incorporating BDP as an additional antenna group in porphyrin structures, new dyes with enhanced overall absorption profiles can be obtained.[47,48] In order to enhance the absorption band in the visible region, a molecular system consists of energy donor and energy acceptors were widely used to design fluorescene resonance energy transfer molecular assemblies.[49-51] Additionally, to maximize the light harvesting ability of such dyes, the two chromophores can also be linked through appropriate linkers. 1,3,5-triazine has been successfully used as linker in metal free organic dyes, which were used as sensitizers in DSSCs and other photoconductive materials.[52-54] The structural, chemical and electronic properties of this moiety allow the design and facile synthesis of complex π-conjugated multi-chromophores,

and offer improved light harvesting ability, as well as electron injection and transportation rates.[55, 56]

Herein, we present the use of a BDP-porphyrin triad bridged by a triazine linker **(PorCOOH)(BDP)$_2$** (Scheme 1) along with the $PC_{71}BM$ (Scheme 1) as electron donor and electron acceptor, respectively, for the fabrication of solution processed BHJ organic solar cells. The solar cell based on **(PorCOOH)(BDP)$_2$**:$PC_{71}BM$ in 1:1 by weight ratio and cast from THF solvent showed an overall PCE value of 3.48 % with J_{sc}= 8.04 mA/cm^2, V_{oc}= 0.94 V and FF =0.46. Remarkably, when the active layer of the solar cell was processed by using a 4% v/v mixture of pyridine /THF as solvent, its photovoltaic characteristics were significantly improved resulting in a PCE value of 5.29%. This was ascribed to an increase in hole mobility, resulting in better values of charge transport and charge collection rates due to the optimized crystallinity and nanoscale morphology of the active layer, induced by the solvent additive.

2. Results and discussion:

Synthesis, Photophysical and Electronic properties of porphyrin triad. As shown in Scheme 1 the porphyrin triad that is used in the present work, **PorCOOH(BDP)$_2$** consists of a meso aryl-substituted free base monocarboxy-porphyrin unit bridged by a central 1,3,5-triazine moiety to 4-aminophenyl-boron dipyrrin units through their aryl amino groups. Its synthetic approach involves the stepwise amination reactions of cyanuric chloride with amino-phenyl monocarboxy porphyrin (**PorCOOH**) and 4-aminophenyl-boron dipyrrin (**NH$_2$-BDP**) in the presence of a weak base (DIPEA).

The optical absorption spectrum of **(PorCOOH)(BDP)$_2$** in dilute THF solution and thin film cast from the THF solvent is shown in Figure 1a. The spectrum of **(PorCOOH)(BDP)$_2$** exhibits the characteristic absorption bands for free-base porphyrin (strong Soret band: λ_{max} = 422 nm, weaker Q- bands: λ_{max}=552 nm, 596 nm and 652 nm) in addition to one more absorption band centered at 502 nm which is attributed to the π-π* transition of BODIPY moiety.[57] The fact that the absorption spectrum appears to be the sum

of the absorption spectra of the porphyrin **PorCOOH** and **BODIPY** moiety, indicates that their connection through the triazine bridge does not cause significant electronic interactions between them in the ground state of the triad. The absorption spectrum of **(PorCOOH)(BDP)$_2$** thin film **(**Figure 1, red line) is similar but with broader bands than those of the solution spectrum, which may be attributed to porphyrin aggregation. The optical bandgap was calculated from the onset absorption edge of band on thin film to be about 1.84 eV.

The HOMO and LUMO energy levels of **(PorCOOH)(BDP)$_2$** were estimated from its first oxidation potential (0.91 V vs SCE) and first reduction potential (-1.19 V vs SCE) and correspond to -5.62 eV and -3.52 eV, respectively. The deeper energy value of HOMO of **(PorCOOH)(BDP)$_2$** is beneficial for the higher value of V_{oc}. Moreover, the LUMO energy level of **(PorCOOH)(BDP)$_2$** is sufficiently higher than that of the $PC_{71}BM$ (~ -4.0 eV) and favorable for the photo-induced charge transfer between **(PorCOOH)(BDP)$_2$** and $PC_{71}BM$.[58]

2.1. Photovoltaic properties

The performance of an organic BHJ solar cells that combines a donor and an acceptor species, is not surprisingly influenced by the relative concentrations of these materials used in the active thin film, as there should be a balance between the absorbance of photons and the subsequent charge transporting process in the active layer. When the concentration of the acceptor material is low, the electron transporting ability will be limited while with the higher amount of acceptor concentration, the absorbance and hole transport ability in the active layer will be decreased. In our system, the optimum device performance was measured in a blend of 1:1 weight ratio of the mixture **(PorCOOH)(BDP)$_2$** and $PC_{71}BM$ in THF, after testing a series of three different weight ratios (1:0.5, 1:1 and 1:1.5). The normalized absorption spectrum of **(PorCOOH)(BDP)$_2$:**$PC_{71}BM$ (1:1) blend (Figure 2) shows the combination of both **(PorCOOH)(BDP)$_2$** and $PC_{71}BM$ absorption features and it becomes obvious that both moieties participate in light absorption and exciton generation, thus photocurrent generation.

The current–voltage (J-V) characteristics under AM 1.5 (100 mW/cm^2) stimulated solar illumination of BHJ organic solar cell with optimized **(PorCOOH)(BDP)$_2$**:$PC_{71}BM$ (1:1 w/w) processed with THF solvent are shown in Figure 3a and photovoltaic parameters are summarized in Table 1. The device showed an overall PCE value of 3.48%, with J_{sc}= 8.05 mA/cm^2, V_{oc} = 0.94 V and FF = 0.46. The respectable value of V_{oc} can be explained by the lower energy of the HOMO of **(PorCOOH)(BDP)$_2$,** since the V_{oc} of the BHJ organic solar cells is directly related to the energy difference between the HOMO of the donor and the LUMO of the acceptor.

The incident photon to current conversion efficiency (IPCE) spectrum of the BHJ organic solar cell based on **(PorCOOH)(BDP)$_2$**:$PC_{71}BM$ (1:1 w/w) is shown in Figure 3b and it closely resembles the optical absorption spectrum of **(PorCOOH)(BDP)$_2$**:$PC_{71}BM$ blended thin film (Figure 2), indicating that both **(PorCOOH)(BDP)$_2$** and $PC_{71}BM$ contribute to the exciton generation after the absorption of photons by the active layer. The IPCE values of both Soret and Q bands are almost similar, which indicates that despite the differences in absorption, all the electronic transitions are equally efficient in converting photons to electrons. Nevertheless, the overall PCE value of the organic solar cell based on **(PorCOOH)(BDP)$_2$**:$PC_{71}BM$ active layer processed from THF is smaller than that reported in the literature when other small molecules are used as donors.[21-25]

Although the V_{oc} of the present device is quite high (V_{oc} = 0.94 V), the lower PCE value is mainly due to the low values of both J_{sc} and FF. These two parameters are directly related to the light harvesting efficiency of active layer and the resulting charge generation as well as to the charge transport and collection to the respective electrodes, processes that depend on the film morphology. A well defined nanomorphology and phase separation between donor and acceptor components in the active layer within the range of exciton diffusion length is necessary for efficient exciton dissociation and charge transport.[59] All the above factors that influence the overall PCE value of our device are explained below.

It is reported that controlling the morphology of active layer, induced by the appropriate treatment methodologies, i.e., thermal annealing,[60,61] solvent annealing[16, 62] and solvent additives,[63-67] the photovoltaic performance of BHJ organic solar cells based on either conjugated polymers or small molecules can be significantly improved. Particularly, the choice of solvent is a main factor and influences greatly the overall PCE value of organic solar cell based on BHJ active layer. Recently, the solvent additive method was used to improve the performance of BHJ organic solar cells using porphyrins as electron donors and $PC_{71}BM$ as electron acceptor with remarkable results.[38,39] Aiming to improve the overall PCE value of our device based on the optimized **PorCOOH(BDP)$_2$**:$PC_{71}BM$ active layer, we have employed the solvent additive treatment method using a small amount of pyridine as solvent additive, as it is known to be more effective than other solvent additives for porphyrin based BHJ solar cells.[38,39] We have added different concentrations of pyridine (1, 2, 3, 4, and 5% v/v) into the host THF solvent and then we tested their photovoltaic perfromance. The optimum efficiency was achieved in concentration 4% v/v pyridine in THF (added to the host THF solvent before the spin coating of active layer). The J-V characteristics of the BHJ solar cell processed with this solvent mixture are shown in Figure 3a while the corresponding photovoltaic parameters are complied in Table 1. The PCE value of the organic solar cell based on BHJ active layer processed with solvent additive was significantly enhanced from 3.48 % to 5.29 % with J_{sc} = 10.48 mA/cm^2, V_{oc} = 0.90 V and FF =0.56. This improvement is due to higher values of both J_{sc} and FF parameters of the device. The improvement in the J_{sc} value is consistent with the IPCE spectra of the device processed with pyridine/THF solvent, i.e. higher values of IPCE throughout the wavelength range (Figure 3b). The J_{sc} values estimated from the integration of IPCE spectra are found to be 7.95 mA/cm^2 and 10.32 mA/cm^2, for the solar cells based on THF and pyridine/THF cast active layer, respectively. These values are consistent with the experimentally observed in J-V characteristics of the respective devices.

In order to investigate the morphology and surface roughness of the active layers processed with and without pyridine additive, atomic force microscopy (AFM) measurements were performed and shown in Figure 4. The root mean square (rms) roughness values were found to be 3.54 nm and 1.26 nm for the active layer processed without and with pyridine solvent additive, respectively. This result indicates that pyridine additive induces the improvement in the phase separation with reduced domain sizes which is beneficial for exciton dissociation and charge transport.

The crystallinity of the active layer also is a key participant in the charge transport and collection, thereby increasing the overall PCE value of the organic solar cell. To get information about the change in the crystallinity of the **(PorCOOH)(BDP)$_2$**:$PC_{71}BM$ film with the addition of pyridine in the host solvent, prior the spin casting, we have recorded the X-ray diffraction (XRD) pattern of the spin cast thin film processed with and without pyridine additive. In addition, we have also recorded the XRD patterns of pristine **(PorCOOH)(BDP)$_2$** thin film cast from THF and pyridine/THF solvents, for comparison (Figure 5a). The pristine **(PorCOOH)(BDP)$_2$** cast from THF as well as from pyridine/THF showsstrong diffraction peak at 2θ=7.12°, but the intensity of the later is stronger than the one of the former, indicating that the crystallinity of the film is increased with the addition of pyridine additive. The blend **(PorCOOH)(BDP)$_2$**:$PC_{71}BM$ cast from THF (black color Figure 5b) also shows a diffraction peak at around 2θ=7.12°, corresponding to **(PorCOOH)(BDP)$_2$** unit but its intensity becomes weak, suggesting an effective mixing of $PC_{71}BM$ and **(PorCOOH)(BDP)$_2$**. However, this diffraction peak becomes more intense in the corresponding blend cast from pyridine/THF solvent, while its width at half maximum height is decreased. These results indicate that the blend film cast from the THF solvent has low crystallinity, while in the case of blend film cast from pyridine/THF solvent, the crystallinity and π conjugation of **(PorCOOH)(BDP)$_2$** in the blend increases. This is probably due to the difference in the

boiling point of THF and pyridine, that makes the spin coated film to dry slowly, assisting in the formation of a better self ordered structure of the blend. The increase in the crystallinity leads to an enhancement in the light absorption property of the active layer and higher hole mobility in the blend film, leading to the increase in J_{sc}, FF and PCE values of the organic solar cell.

The difference in PCE value of the solar cell, when the active layer was spin cast from pyridine/THF solution, may be the diiference in exction dissociation efficiency, after the exction generation. Photoluminenscene (PL) quenching provides direct evidence for the exciton dissociation, which inflences the J_{sc} and is used as a measure of photoinduced charge transfer between donor and acceptor interface present in the active layer. PL was measured to investigate the exciton dissociation efficiency. Figure 6 shows the PL spectra of spin coated (**PorCOOH)(BDP)$_2$** (THF cast) and **PorCOOH)(BDP)$_2$:**$PC_{71}BM$ (1:1) (THF and pyridine/THF cast) blend films. As can be seen from this figure that pristine **PorCOOH)(BDP)$_2$** showed displayed PL with a peak aroud 664 nm. Blending **PorCOOH)(BDP)$_2$** with $PC_{71}BM$, the PL peak is quenched. The degree of quenching is more with the addition of pyridine. This effective PL quenching suggests that the exciton seperation was highly efficient in the active layer cast from pyridine/THF as compared to that for THF cast active layer. The more effective quenching in the pyridine/THF cast film than in THF cast film implies two possibilites: (i) better exciton dissociation in the pyridine /THF cast film, (ii) a larger interfacial area between the **PorCOOH)(BDP)$_2$** and $PC_{71}BM$ through the optimal nanoscale phase seperation. The former could be ruled out, because this is mainly energy difference between the HOMO of the donor and LUMO of the acceptor used in the blend. The second mechanism is mainly responsible for the effective PL quenching as confirmed from the active layer film morphology studies. Thus the optimized phase seperation and crystallinity of the active layer are important factor for efficient exciton dissociation. The

morphology and quenching of PL intensity revealed that the active layer processed with pyridine/THF exhibits more favorable features for higher J_{sc}.

We further studied the effect of pyridine on the charge generation in the **(PorCOOH)(BDP)$_2$**:$PC_{71}BM$ BHJ solar cells by investigating the saturation point where the internal field is large enough to sweep out all the carriers to the electrodes prior to recombination. Figure 6 shows the variation of photocurrent density (J_{ph}) with the internal voltage (V_{int}) of the device processed with and without additive, under illumination at 100 mW/cm^2. J_{ph} value is estimated as $J_{ph}=J_L-J_d$, where J_L and J_d are the current density under illumination and in the dark, respectively.[68] V_{int} value is determined as $V_{int}=V_o-V$, where V_o is the voltage at which J_{ph} value is zero and V is the applied voltage.[69,70] Therefore, V_{int} corresponds to the strength of electric field within the device to extract the charge carriers. As it can be seen from Figure 6, J_{ph} value increases linearly with voltage at low V_{int}, but saturates at high V_{int} (1.8 V or higher). Therefore, we assume that almost all the photogenerated charge carriers within the device are collected at high V_{int} and J_{ph} saturated and independent of V_{int}. The J_{ph} at V_{int} = 3.2 V is found to be at about 12 mA/cm^2 and 9.8 mA/cm^2 for the devices, processed with and without pyridine additive, respectively, suggesting that the charge generation in the devices is influenced by the solvent additives. The charge collection probability (P_c) of the solar cells based on the active layers processed with and without pyridine additive, were estimated as $P_c = J_{sc}/ J_{ph,sat}$, and were found to be about 0.87 and 0.78, respectively. The low charge generation could be explained in terms of deficient photon absorption and /or charge separation. Concerning the former parameter, the UV-visible absorption bands of **(PorCOOH)(BDP)$_2$**:$PC_{71}BM$ BHJ active layer processed with pyridine additive are stronger than the corresponding processed without additive (see Figure 2) proving that there is indeed a difference in photon absorption. Nevertheless, the charge separation is another significant parameter that cannot be neglected, as there is a difference between the two devices in terms of domain size of the phase separation, as confirmed by AFM images,

which is critical to charge recombination. So as the excitons are generated away from the D/A interfaces, they are not able to reach the interfaces in the large domain size of phase separation in the device processed in THF and the chances of recombination before the excitons are dissociated into free charge carriers, are increased. However, the solvent additive reduces this domain size and increases the D/A interfacial area, so that, more excitons are dissociated into free charge carriers.

The charge carrier mobility in the BHJ active layer is critical in the BHJ organic solar cell efficiency because the photogenerated charges extract at the electrode depends on the competition between carrier sweep out, which is limited by the carrier mobility, and the loss of photogenerated carriers by recombination.[69,70] The hole and electron mobility of optimized **(PorCOOH)(BDP)$_2$**:$PC_{71}BM$ BHJ active layer processed with and without pyridine additive were estimated by space charge limited current (SCLC) method (J-V characteristics in dark) using the hole only device (ITO/PEDOT:PSS/ **(PorCOOH)(BDP)$_2$**:$PC_{71}BM$/Au) and the electron only device (ITO/Al/**(PorCOOH)(BDP)$_2$**:$PC_{71}BM$/Al), respectively. The results were analyzed using the SCLC model described by Mott-Gurney law which includes a small field dependent term, as seen in following equation.[71-73]

$$J = \frac{9}{8}\varepsilon_r \varepsilon_o \mu_o \frac{(V_{app} - V_{bi})^2}{L^3} \exp\left(\beta \sqrt{\frac{V_{app} - V_{bi}}{L}}\right)$$

Where $\varepsilon_r\varepsilon_o$is the dielectric permittivity of the active layer, L is the thickness of the active layer, V_{app} is the applied voltage, $V_{bi}$is the built in voltage, μ_o is the zero field mobility, and β is the field activation factor.

The J-V characteristics of the hole only device in dark were shown in Figure 7. The fitting of the experimental results (solid lines) revealed that the hole mobilities are found to be 8.5 x10^{-6} cm^2/Vs and 8.15 x10^{-5} cm^2/Vs for the device without and with pyridine additives, respectively. The increase in the pyridine additives agrees well with the results revealed by

the morphology analysis, in which the domain size and crystallinity decreases and increases, respectively with the pyridine additives. The electron mobility of the active layer processed with and without pyridine additive are quite similar, i.e. 2.29 x10^{-4} cm^2/Vs and 2.34 x10^{-4} cm^2/Vs, respectively. The ratios of electron to hole mobilities in the active layer processed with and without additive were found to be about 2.80 and 27.53, respectively. Therefore it seems that in the active layer processed with pyridine, the charge carrier transports in donor (holes) and acceptor (electrons) phase are more balanced as compared to active layer proceesed without pyridine, a feature that increases J_{sc} and FF values, of the device, leading to a higher overall PCE value.

We finally investigated the variation of J_{sc} as a function of illumination intensity to gain insight into the charge recombination kinetics occurring in the device. The dependence of J_{sc} on the light intensity is shown in Figure 8, in which the data (open circles) are plotted in log-log scale and fitted to a power law (solid lines). Generally, a power law dependence of J_{sc} upon light intensity (I) is observed in organic solar cells, i.e. $J_{sc} \propto I^{\gamma}$. For an ideal solar cell, the exponential factor (γ) must be unity which is indicative of efficient sweep out of carriers prior to recombination.[74-76] From Figure 8, we have extracted the values of exponential factor for the devices processed with and without pyridine additives and were found to be 0.93 and 0.84, respectively. The increase in the exponential factor i.e. closer to unity for the device processed with pyridine additive implies that the sweep out and extraction of charge carriers is more efficient in this device as compared to the device processed without additive. This is in agreement with the balanced charge transport observed from the mobility measurement. The deviation from $\gamma = 1$ in device based on the active layer processed without additive suggests that the bimolecular recombination is more important in this device. An unbalanced hole and electron mobilities in this device, as discussed earlier, can also be attributed to the deviation of γ value from unity.

We have estimated the series resistance (R_s) and shunt resistance (R_{sh}) from the slope of the J-V characteristics of devices, under illumination, around the V_{oc} and J_{sc}, respectively and complied in Table 1. In general, the R_s of the organic solar cell is composed of the bulk resistance of the active layer depends on the charge transport ability within the active layer and morphology of the active layer. It can be seen from the table 1 that R_s of the device processed with pyridine/THF solvent is significantly lower than that for processed with THF, and may be attributed to better morphology and balanced charge transport. Therefore, higer boiling point of pyridine offers more time for the adjustment of molecular aggregation to improve the morphology and interpentrating pathways network for charge transport, reducing the R_s and increasing the J_{sc} and FF.[77] The increase in R_{sh} is related to the decrease in leakage current and depends on the intermolecular interaction (or electronic) coupling between the donor and acceptor materials in the active layer. Therefore, the slight decrease in the V_{oc} value for the device processed with addtive could be due to the increasing intermolecular interaction between the donor and acceptor.

3. Conclusion

In this report we presented the use of **(PorCOOH)(BDP)$_2$** as electron donor for the fabrication of solution processed BHJ solar cells, along with $PC_{71}BM$ as electron acceptor. The optical and electrochemical properties of **(PorCOOH)(BDP)$_2$** suggest that **(PorCOOH)(BDP)$_2$:**$PC_{71}BM$ blend can effectively harvest photons and transfer electrons from **(PorCOOH)(BDP)$_2$** to $PC_{71}BM$, resulting in a photovoltaic effect. The solar cell based on a **(PorCOOH)(BDP)$_2$**:$PC_{71}BM$ BHJ active layer with optimized 1:1 weight ratio, processed with THF, displayed a PCE value of 3.48%. In order to improve the efficiency of this organic solar cell, the **(PorCOOH)(BDP)$_2$**:$PC_{71}BM$ BHJ active layer was processed with a solvent mixture of 4% v/v of pyridine in THF. The PCE value of the resulting solar cell was improved up to 5.29%, as a result of the enhancement of its J_{sc} and FF values, parameters that are related to the charge generation/separation/mobility/transport that are found to be

significantly improved by the morphology and crystallinity change of the active layer upon addition of pyridine.

4. Experimental Section

General Methods and Materials. All synthetic manipulations were carried out using standard Schlenk techniques under nitrogen atmosphere. 2,4,6-Trichloro-1,3,5-triazine (cyanuric chloride), diisopropylamine (DIPEA), $PC_{71}BM$, and other chemicals and solvents were purchased from usual commercial sources and used as received, unless otherwise stated. 4-Aminophenyl-boron dipyrrin (BDP) and 5-(4-carboxyphenyl)-15-(4-aminophenyl)-10,20-bis(2,4,6-trimethylphenyl)-porphyrin (PorCOOH) and triad **PorCOOH(BDP)$_2$** were prepared according to literature procedures.[78,79] Tetrahydrofurane (THF) was freshly distilled from Na/benzophenone.

Photophysical Measurements. UV−vis absorption spectra were measured on a Shimadzu UV-1700 spectrophotometer using 10 mm path-length cuvettes.

Solar Cell Fabrication. The BHJ organic solar cells were fabricated using the glass/ITO/PEDOT:PSS/PPT:$PC_{71}BM$/Al device architecture. The indium tin oxide (ITO) patterned substrates were cleaned by ultrasonic treatment in aqueous detergent, deionized water, isopropyl alcohol, and acetone sequentially, and finally dried under ambient conditions. The anode consisted of glass substrates percolated with ITO, modified by spin coating with a PEDOT:PSS layer (60 nm) as hole transport and heated for 10 min at 100°C. Mixtures of **(PorCOOH)(BDP)$_2$** with $PC_{71}BM$ with weight ratios of 1:0.5, 1:1, and 1:1.5 in THF were prepared and then spin-cast onto the PEDOT:PSS layer and dried overnight at ambient atmosphere. For the **(PorCOOH)(BDP)$_2$**:PC_{71} BM blend processed with 1, 2, 3, 4% and 5 % v/v of pyridine in THF solvent mixture only the 1:1 weight ratio mixture was used. The total concentration of mixture was 10 mg/mL for each active layer. The approximate thickness of the active layers was 90 nm. Finally, the aluminum (Al) top electrode was thermally deposited on the active layer at a vacuum of 10^{-5} Torr through a shadow mask of area of 0.20 mm^2. All

devices were fabricated and tested in ambient atmosphere without encapsulation. The hole-only and electron-only devices with ITO/PEDOT:PSS/**(PorCOOH)(BDP)$_2$**:$PC_{71}BM$/Au and ITO/Al/**(PorCOOH)(BDP)$_2$**:$PC_{71}BM$/Al architectures were also fabricated in a similar way, in order to measure the hole and electron mobility, respectively.

Photovoltaic Measurements. The current-voltage (J-V) characteristics of the BHJ organic solar cells were measured using a computer controlled Keithley 238 source meter in dark and under simulated AM 1.5G illumination of 100 mW/cm^2. A xenon light source coupled with optical filter was used to give the stimulated irradiance at the surface of the devices. The incident photon to current efficiency (IPCE) of the devices was measured illuminating the device through the light source and monochromator and the resulting current was measured using a Keithley electrometer under short circuit condition.

X-ray Powder Diffraction measurements. XRD measurements were recorded on a Bruker D8 Advanced model diffractometer with Cu Kα radiation (λ = 1.542 Å) at a generator voltage of 40 kV.

Acknowledgements

Financial support from the European Commission (FP7-REGPOT-2008-1, Project BIOSOLENUTI No. 229927) is greatly acknowledged. This research has also been co-financed by the European Union (European Social Fund) and Greek national funds (Heraklitos II) through the Operational Program "Education and Lifelong Learning" of the National Strategic Reference Framework Research Funding Program (THALIS-UOA-MIS 377252).

(1). J. Chen, Y. Cao, *Acc. Chem. Res.,* 2009, **42**, 1709-1718.
(2). Y. J. Cheng, S. H. Yang, C. S. Hsu, *Chem. Rev.,* 2009, **109**, 5868-5923.
(3). G. Li, R. Zhu, Y. Yang, *Nat. Photonics,* 2012, **6**, 153-161.
(4). Y. Li, *Acc. Chem. Res.,* 2012, **45**, 723-733.
(5). Z. He, S. Su, M. Xu, H. Wu, Y. Cao, *Nat. Photonics,* 2012, **6**, 591-595.
(6). S.-H. Liao, H.-J. Jhuo, Y.-S. Cheng, S.-A. Chen, *Adv. Mater.,* 2013, **25**, 4766-4771.
(7). L. Dou, J. You, Z. Hong, Z. Xu, G. Li, R. Street, Y. Yang, *Adv. Mater.,* 2013, **25**, 6642-6671.
(8). Subbiah, J.; Purushothaman, B.; Chen, M.; Qin, T.; Gao, M.; Vak, D.; Scholes, F. H.; X. Chen, S. E. Watkins, G. J. Wilson, A. B. Holmes, W. W. H. Wong, D. J. Jones, *Adv. Mater.*, 2015, **27**, 702-705.
(9). J. B. You, L. T. Dou, K. Yoshimura, T. Kato, K. Ohya, T. Moriarty, K. Emery, C. C. Chen, J. Gao, G. Li, Y. Yang, *Nat. Commun.,* 2013, **4**, 1446-1455.
(10). J. B. You, C. C. Chen, Z. R. Hong, K. Yoshimura, K. Ohya, R. Xu, S. L. Ye, J. Gao, G. Li, Y. Yang, *Adv. Mater.,* 2013, **25**, 3973-3978.
(11). Y. S. Liu, C. C. Chen, Z. R. Hong, J. Gao, Y. Yang, H. P. Zhou, L. T. Dou, G. Li, Y. Yang, *Sci. Rep.,* 2013, **3**, 3356-3364.
(12). J.-D. Chen, C. Cui, Y.-Q. Li, L. Zhou, Q.-D. Ou, C. Li, Y. Li, J.-X. Tang, *Adv. Mater.,* 2015, **27**, 1035-1041.
(13). Y. Lin, Y. Li, X. Zhan, *Chem. Soc. Rev.,* 2012, **41**, 4245-4272.
(14). A. Mishra, P. Bauerle, *Angew. Chem., Int. Ed.,* 2012, **51**, 2020-2067.
(15). J. Roncali, *Acc. Chem. Res.,* 2009, **42**, 1719-1730.
(16). Y. Chen, X. Wan, G. Long, *Acc. Chem. Res.,* 2013, **46**, 2645-2655.
(17). T. S. van der Poll, J. A. Love, T.-Q. Nguyen, G. C. Bazan, *Adv. Mater.,* 2012, **24**, 3646-3649.
(18). J. Zhou, X. Wan, Y. Liu, Y. Zuo, Z. Li, G. He, G. Long, W. Ni, C. Li, X. Su, Y. Chen, *J. Am. Chem. Soc.,* 2012, **134**, 16345-16351.
(19). Z. Li, G. He, X. Wan, Y. Liu, J. Zhou, G. Long, Y. Zuo, M. Zhang, Y. Chen, *Adv. Energy Mater.,* 2012, **2**, 74-77.
(20). Y. Sun, G. C. Welch, W. L. Leong, C. J. Takacs, G. C. Bazan, A. J. Heeger, *Nat. Mater.,* 2011, **11**, 44-48.
(21). J. Zhou, Y. Zuo, X. Wan, G. Long, Q. Zhang, W. Ni, Y. Liu, Z. Li, G. He, C. Li, B. Kan, M. Li, Y. Chen, *J. Am. Chem. Soc.,* 2013, **135**, 8484-8487.
(22). A. K. K. Kyaw, D. H. Wang, D. Wynands, J. Zhang, T.-Q. Nguyen, G. C. Bazan, A. J. Heeger, *Nano Lett.,* 2013, **13**, 3796-3801.
(23). Q. Zhang, B. Kan, F. Liu, G. Long, X. Wan, X. Chen, Y. Zuo, W. Ni, H. Zhang, M. Li, Z. Hu, F. Huang, Y. Cao, Z. Liang, M. Zhang, T. P. Russell, Y. Chen, *Nature Photonics,* 2015, **9**, 35-41.
(24). B. Kan, Q. Zhang, M. Li, X. Wan, W. Ni, G. Long, Wang, X. Yang, H. Feng, Y. Chen, *J. Am. Chem. Soc.,* 2014, **136**, 15529-15532.
(25). V. Gupta, A. K. K. Kyaw, D. H. Wang, S. Chand, G. C. Bazan, A. J. Heeger, *Scientific Reports,* 2013, **3**, 1965-1970 (DOI: 10.1038/srep01965)
(26). C. W. Tang, A. C. Albrecht, *Nature,* 1975, **254**, 507-509.
(27). A. Goetzberger, C. Hebling, H. W. Schock, *Mater. Sci. Eng.,* 2003, **R40**, 1-46.
(28). C. W. Lee, H. P. Lu, C. M. Lan, Y. L. Huang, Y. R. Liang, W. N. Yen, Y. C. Liu, Y. S. Lin, E. W. G. Diau, C. Y. Yeh, *Chem.–Eur. J.,* 2009, **15**, 1403-1412.
(29). C. L. Mai, W. K. Huang, H. P. Lu, C. W. Lee, C. L. Chiu, Y. R. Liang, E. W. G. Diau, C. Y. Yeh, *Chem. Commun.,* 2010, **46**, 809-811.

(30). S. Mathew, A. Yella, P. Gao, R. Humphry-Baker, B. F. E. Curchod, N. Ashari-Astani, I. Tavernelli, U. Rothlisberger, M. K. Nazeeruddin, M. Grätzel, *Nat. Chem.,* 2014, **6**, 242-247.
(31). K. Ladomenou, T. N. Kitsopoulos, G. D. Sharma, A. G. Coutsolelos, *RSC Adv.,* 2014, **4**, 21379-21404.
(32). A. Yella, H. W. Lee, H. N. Tsao, C. Yi, A. K. Chandiran, M. K. Nazeeruddin, E. W. G. Diau, C. Y. Yeh, S. M. Zakeeruddin, M. Grätzel, *Science,* 2011, **334**, 629-634.
(33). M. Urbani, M. Grätzel, M. K. Nazeeruddin, T. Torres, *Chem. Rev.,* 2014, **114**, 12330-12396.
(34). J. Hatano, N. Obata, S. Yamaguchi, T. Yasuda, Y. Matsuo, *J. Mater. Chem.,* 2012, **22**, 19258-19263.
(35). Y. Huang, L. Li, X. Peng, J. Peng, Y. Cao, *J. Mater. Chem.,* 2012, **22**, 21841-21844.
(36). L. Li, Y. Huang, J. Peng, Y. Cao, X. Peng, *J. Mater. Chem. A,* 2013, **1**, 2144-2150.
(37). G. D. Sharma, D. Daphnomili, S. Biswas, A. G. Coutsolelos, *Org. Electron.,* 2013, **14**, 1811-1819.
(38). H. Qin, L. Li, F. Guo, S. Su, J. Peng, Y. Cao, X. Peng, *Energy Environ. Sci.,* 2014, **7**, 1397-1401.
(39). C. V. Kumar, L. Cabau, E. N. Koukaras, G. D. Sharma, E. Palomares, *Nanoscale,* 2015, **7**, 179-189.
(40). G. D. Sharma, G. E. Zervaki, P. A. Angaridis, T. N. Kitsopoulos, A. G. Coutsolelos, *J. Phys. Chem. C,* 2014, **118**, 5968-5977.
(41). YI.H. Chao, J.-F. Jheng, J.-S. Wu, K.-Y. Wu, H.-H. Peng, M.-C. Tsai, C.-L. Wang, Y.-N. Hsiao, C.-L. Wang, C.-Y. Lin, C.-S. Hsu, *Adv. Mater.,* 2014, **26**, 5205-5210.
(42). A. Tsuda, A. Osuka, *Science,* 2001, **293**, 79-82.
(43). T. Iekda, N. Aratani, A. Osuka, *Chem. Asian J.,* 2009, **4**, 1248-1256.
(44). Z. Kostereli, T. Ozdemir, O. Buyukcakir, E. U. Akkaya, *Org. Lett.,* 2012, **14**, 3636-3639.
(45). S. Kolemen, O. A. Bozdemir, Y. Cakmak, E. U. Akkaya, *Chem. Sci.,* 2011, **2**, 949-954.
(46). T. Zhang, X. Zhu, W.-K. Wong, H.-L. Tam, W.-Y. Wong, *Chem.– Eur. J.,* 2013, **19**, 739-748.
(47). T. K. Khan, M. Bröring, S. Mathur, M. Ravikanth, *Coord. Chem. Rev.,* 2013, **257**, 2348-2387.
(48). B. Brizet, A. Eggenspiller, C. P. Gros, J.-M. Barbe, C. Goze, F. Denat, P. D. Harvey, *J. Org. Chem.,* 2012, **77**, 3646-3650.
(49). F. Li, S. I. Yang, Y. Cirinhj, J. Seth, C. H. Martin, D. L. Singh, D. Kim, R. R. Birge, D. F. Bocian, D. Holten, J. S. Lindsey, *J. Am. Chem. Soc.,* 1998, **120**, 10001-10017
(50). S. Guo, L. Ma, J. Zhao, B. Kucukoz, A. Karatay, M. Hayvali, H. G. Yaglioglu, A. Elmali, *Chem. Sci*., 2014, **5**, 489-500
(51). J. Zhao, W. Wu, J. Sun, S. Guo, *Chem. Soc. Rev*., 2013, **42**, 3523-5351
(52). H. Zhong, E. Xu, D. Zeng, J. Du, J. Sun, S. Ren, B. Jiang, Q. Fang, *Org. Lett.,* 2008, **10**, 709-712.
(53). J.-W. Kang, D.-S. Lee, H.-D. Park, Y.-S. Park, J.-W. Kim, W.-I. Jeong, K.-M. Yoo, K. Go, S.-H. Kim, J.-J. Kim, *J. Mater. Chem.,* 2007, **17**, 3714-3719.
(54). A. P. Kulkarni, C. J. Tonzola, A. Babel, S. A. Jenekhe, *Chem. Mater.,* 2004, **16**, 4556-4573.
(55). S. Ren, D. Zeng, H. Zhong, Y. Wang, S. Qian, Q. Fang, *J.Phys. Chem. B,* 2010, **114**, 10374-10383.
(56). H. Zhong, H. Lai, Q. Fang, *J. Phys. Chem. C,* 2011, **115**, 2423-2427.
(57). J. Karolin, L. B. A. Johansson, L. Strandberg, T. Ny, *J. Am. Chem. Soc.,* 1994, **116**, 7801-7806.

(58). C. J. Brabec, C. Winder, N. S. Sariciftci, J. C. Hummelen, A. Dhanabalan, P. A. van Hal, R. A. J. Janssen, *Adv. Funct. Mater.,* 2002, **12**, 709-712.
(59). Y. Li, *Acc. Chem. Res.,* 2012, **45**, 723-733.
(60). W. Ma, C. Yang, X. Gong, K. Lee, A. J. Heeger, *Adv. Funct. Mater.,* 2005, **15**, 1617-1622.
(61). J. A. Mikroyannidis, A. N. Kabanakis, S. S. Sharma, G. D. Sharma, *Adv. Funct. Mater.,* 2011, **21**, 746-755.
(62). J. E. Coughlin, Z. B. Henson, G. C. Welch, G. C. Bazan, *Acc. Chem. Res.,* 2013, **47**, 257-270.
(63). J. Peet, J. Y. Kim, N. E. Coates, W. L. Ma, D. Moses, A. J. Heeger, G. C. Bazan, *Nat. Mater.,* 2007, **6**, 497-500.
(64). M. S. Su, C. Y. Kuo, M. C. Yuan, U. S. Jeng, C. J. Su, K. H. Wei, *Adv. Mater.,* 2011, **23**, 3315-3319.
(65). A. Tamayo, T. Kent, M. Tantitiwat, M. A. Dante, J. Rogers, T. Q. Nguyen, *Energy Environ. Sci.,* 2009, **2**, 1180-1186.
(66). H. Fan, H. Shang, Y. Li, X. Zhan, *Appl. Phys. Lett.,* 2010, **97**, 133302/1-133302/3.
(67). B. Walker, C. Kim, T. Q. Nguyen. *Chem. Mater.,* 2011, **23**, 470-482.
(68). S. R. Cowan, A. Roy, A. J. Heeger. *Phys. Rev. B,* **2010**, *82*, 245207/1-245207/10.
(69). S. R. Cowan, R. A. Street, S. Cho, A. J. Heeger, *Phys. Rev. B,* 2011, **83**, 035205/1-035205/8.
(70). A. K. K. Kyaw, D. H. Wang, C. Luo, Y. Cao, T.-Q. Nguyen, G. C. Bazan, A. J. Heeger, *Adv. Energy Mater.,* 2014, **4**, 1301469-1301477.
(71). P. N. Murgatroyd*, Phys. D: Appl. Phys.,* 1970, **3**, 151-156.
(72). V. D. Mihailetchi, H. X. Xie, B. de Boer, L. J. A. Koster, P. W. M. Blom, *Adv. Funct. Mater.,* 2006, **16**, 699-708.
(73). S. M. Tuladhar, D. Poplavskyy, S. A. Choulis, J. R. Durrant, D. D. C. Bradley, J. Nelson, *Adv. Funct. Mater.* **2005**, **15**, 1171-1182.
(74). I. Riedel, J. Parisi, V. Dyakonov, L. Lutsen, D. Vanderzande, J. C. Hummelen, *Adv. Funct. Mater.,* 2004, **14**, 38-44.
(75). P. Schilinsky, C. Waldauf, C. J. Brabec, *Appl. Phys. Lett.* 2002, **81**, 3885-3887.
(76). J. K. J. van Duren, X. Yang, J. Loos, C. W. T. Bulle-Lieuwma, A. B. Sieval, J. C. Hummelen, R. A. J. Janssen, *Adv. Funct. Mater.,* 2004, **14**, 425-434.
(77). J. Huang, C. Zhan, X. Zhang, Y. Zhao, Z. Lu. H. Jai, B. Jiang, J. Ye, S. Zhang, A. Tang, Y. Liu, Q. Pei, J. Jao, *ACS Appl. Mater. Interface,* 2013, **5**, 2030-2039
(78). T. Lazarides, G. Charalambidis, A. Vuillamy, M. Réglier, E. Klontzas, G. Froudakis, S. Kuhri, D. M. Guldi, A. G. Coutsolelos, *Inorg. Chem.,* 2011, **50**, 8926–8936.
(79). G. E. Zervaki, E. Papastamatakis, P. A. Angaridis, M. Singh, R. Kurchania, G. D. Sharma, A. G. Coutsolelos, *Eur. J. Inorg. Chem.*, 2014, 1020-1033.
(80). G. E. Zervaki, A. Nikiforou, V. Nikolaou, G. D. Sharma, G. A. Coutsolelos, in press to *J. Mater. Chem. C,* 2015.

Table 1. Photovoltaic parameters of the BHJ organic solar cells based on active layers of **(PorCOOH)(BDP)$_2$:**$PC_{71}BM$ in 1:1 weight ratio, processed with THF and pyridine(4% v/v)/THF solvents.

Solvent	J_{sc} (mA/cm^2)	V_{oc} (V)	FF	PCE (%)	R_s (Ohm cm^2)	R_{sh} (Ohm cm^2)
THF	8.04	0.94	0.46	3.48[a] (3.36)[b]	53	483
Pyridine (4%v/v)/THF	10.48	0.90	0.56	5.29[a] (5.18)[b]	29.4	594

[a]best result
[b]average of five devices

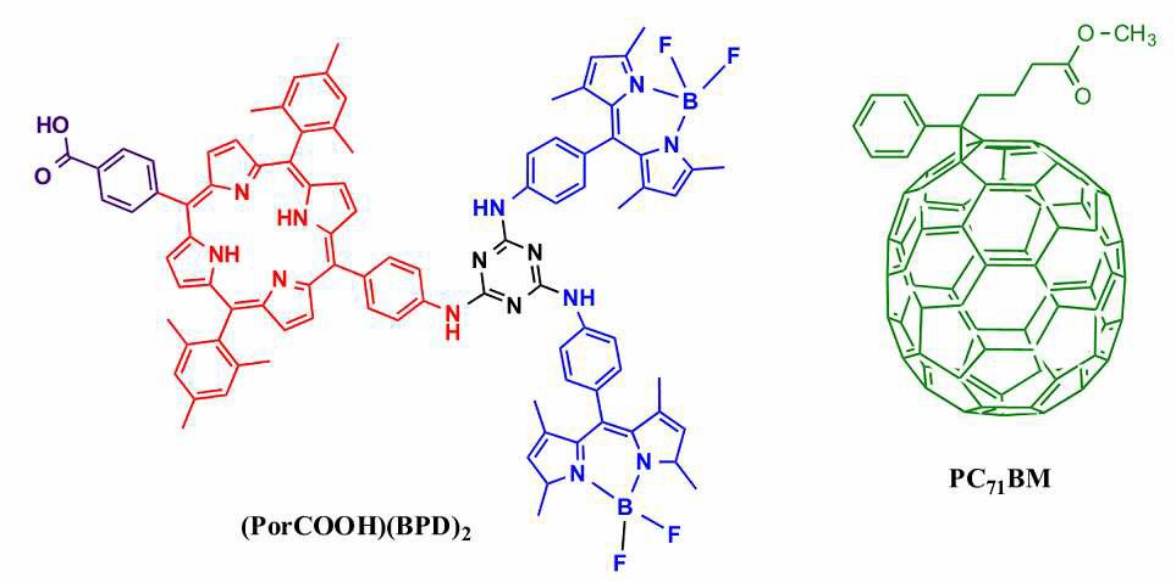

Scheme 1. Chemical structures of **(PorCOOH)(BDP)$_2$** and $PC_{71}BM$.

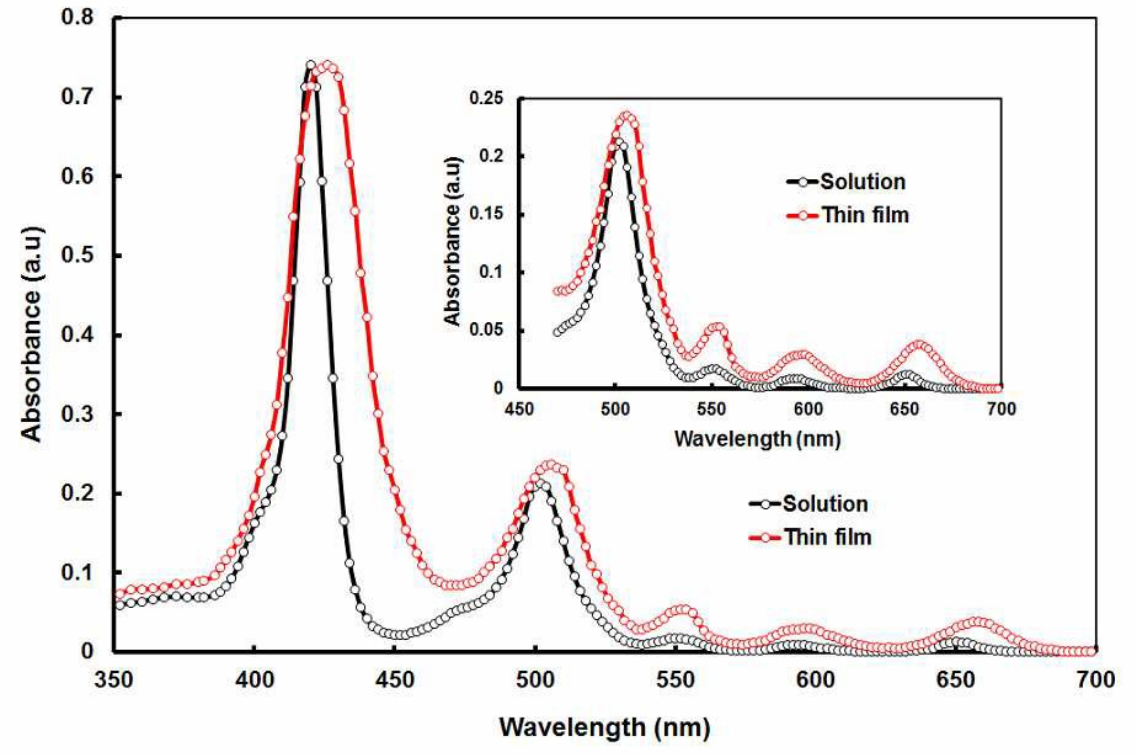

Figure 1. Optical absorption spectra of **(PorCOOH)(BDP)$_2$** in THF solution and thin film cast from the THF solvent.

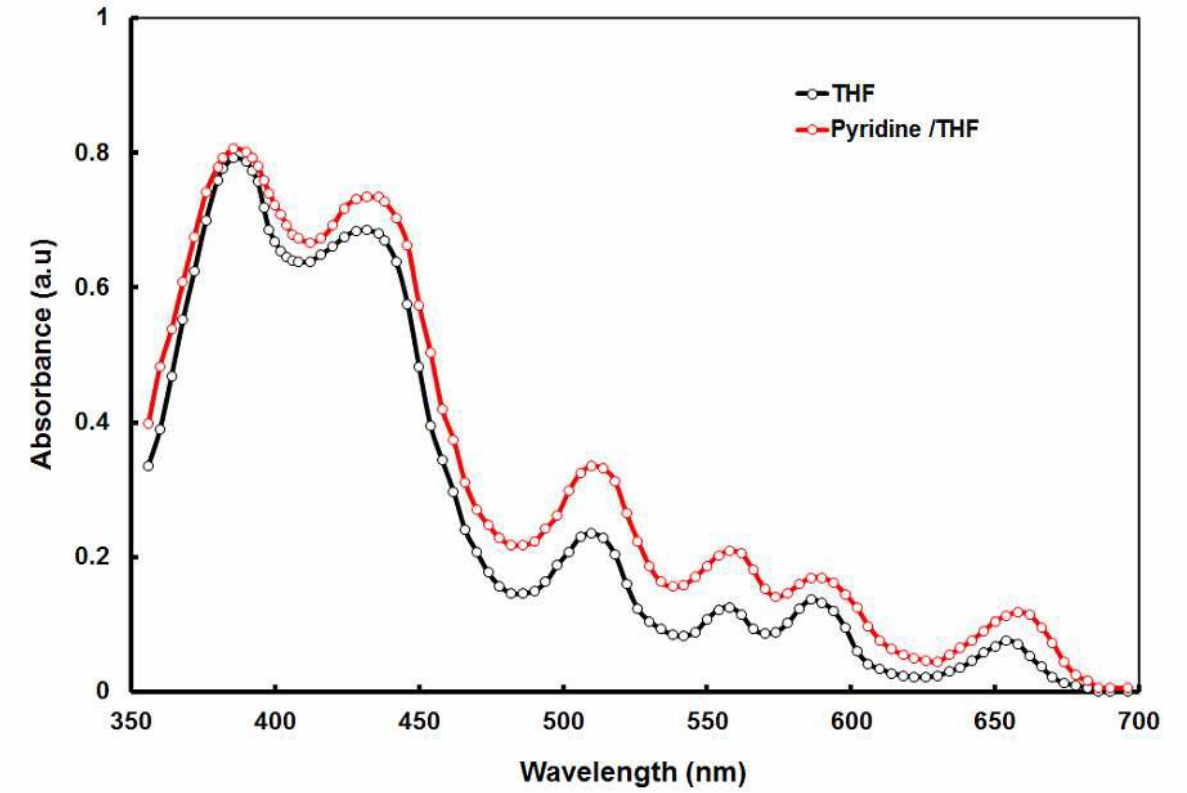

Figure 2: Optical absorption spectra of the **(PorCOOH)(BDP)$_2$**:$PC_{71}BM$ thin film cast from THF and pyridine/THF solvents.

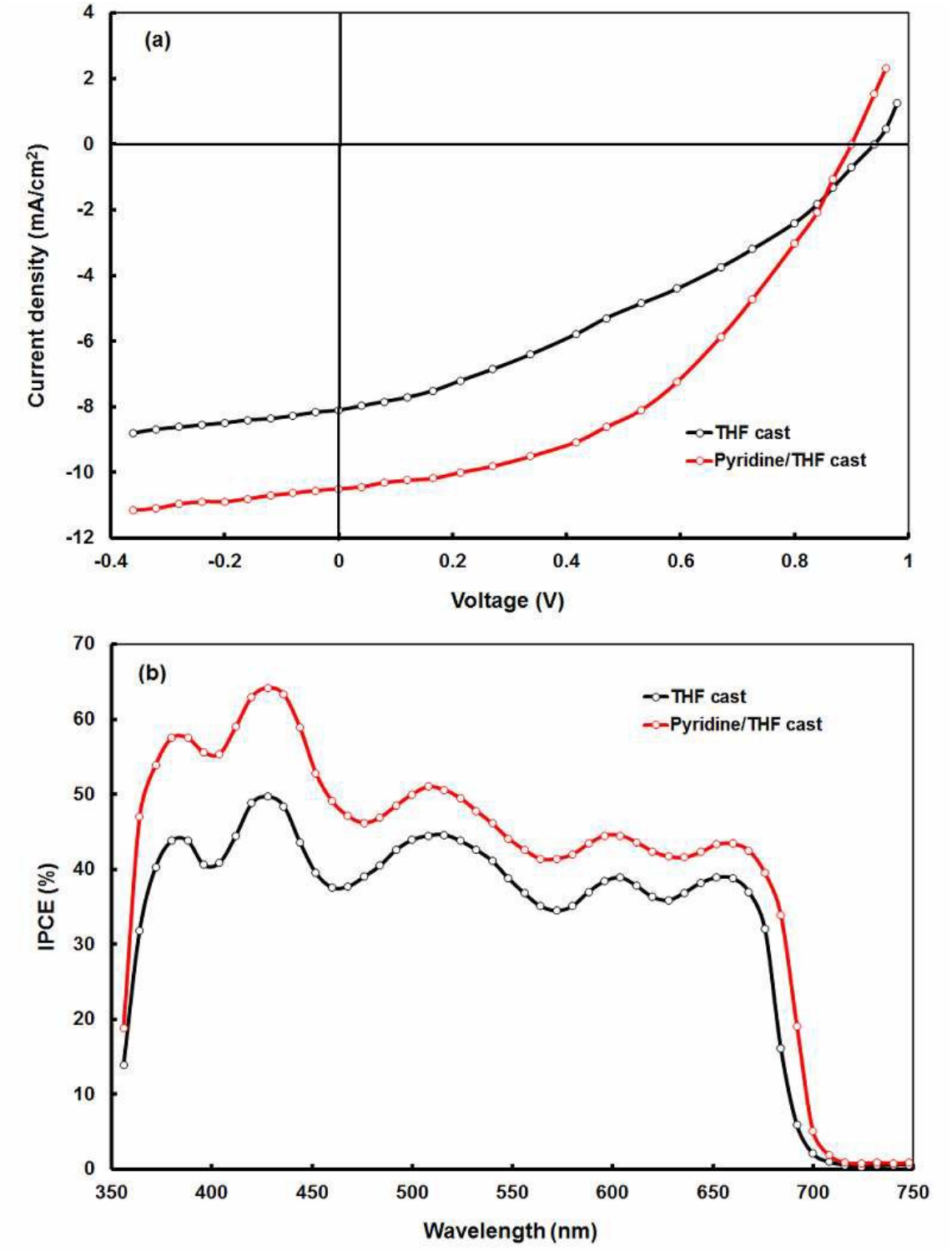

Figure 3: (a) Current–voltage (J–V) characteristics under illumination and (b) IPCE spectra of the BHJ organic solar cells based on differently processed active layers of **(PorCOOH)(BDP)$_2$**:$PC_{71}BM$.

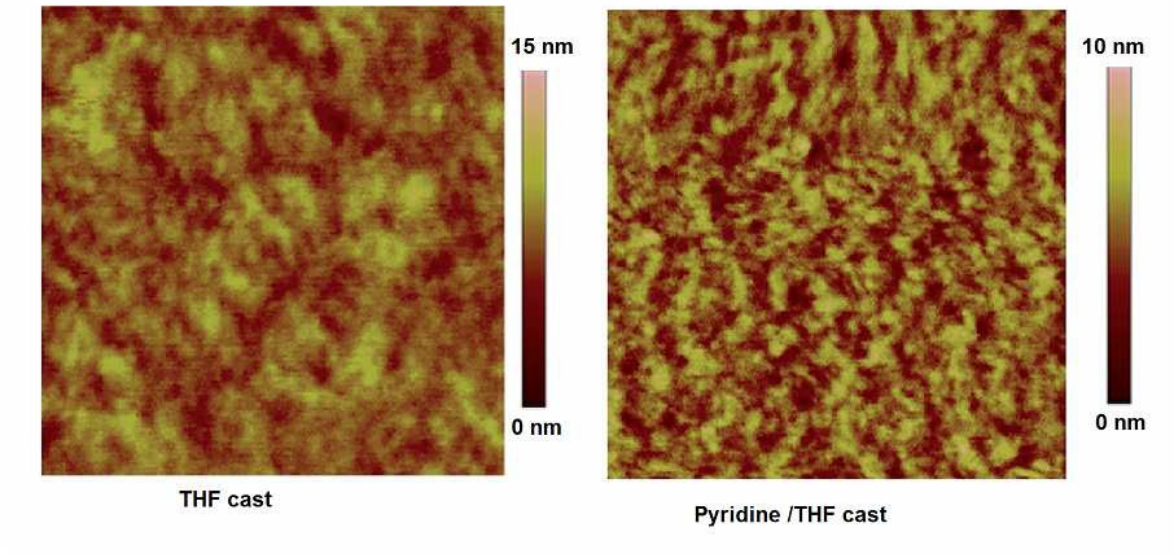

Figure 4: AFM images of **(PorCOOH)(BDP)$_2$**:$PC_{71}BM$ 1:1 blend thin films processed with and without pyridine additives. Image size 3 μm x μm.

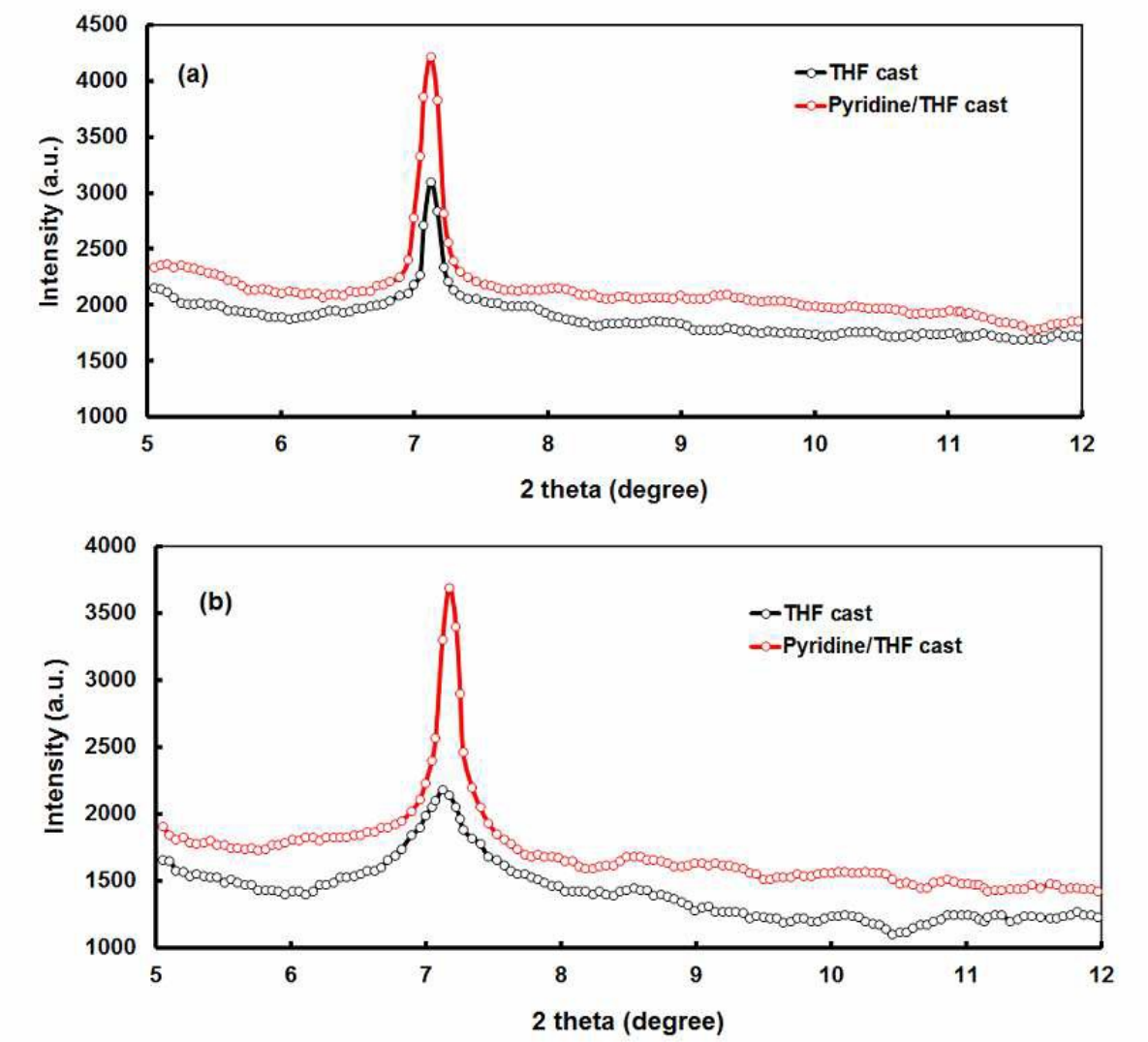

Figure 5: X-ray diffraction (XRD) pattern of (a) pristine **(PorCOOH)(BDP)$_2$ and (b) (PorCOOH)(BDP)$_2$**:$PC_{71}BM$ blend films cast from THF and pyridine/THF solvents.

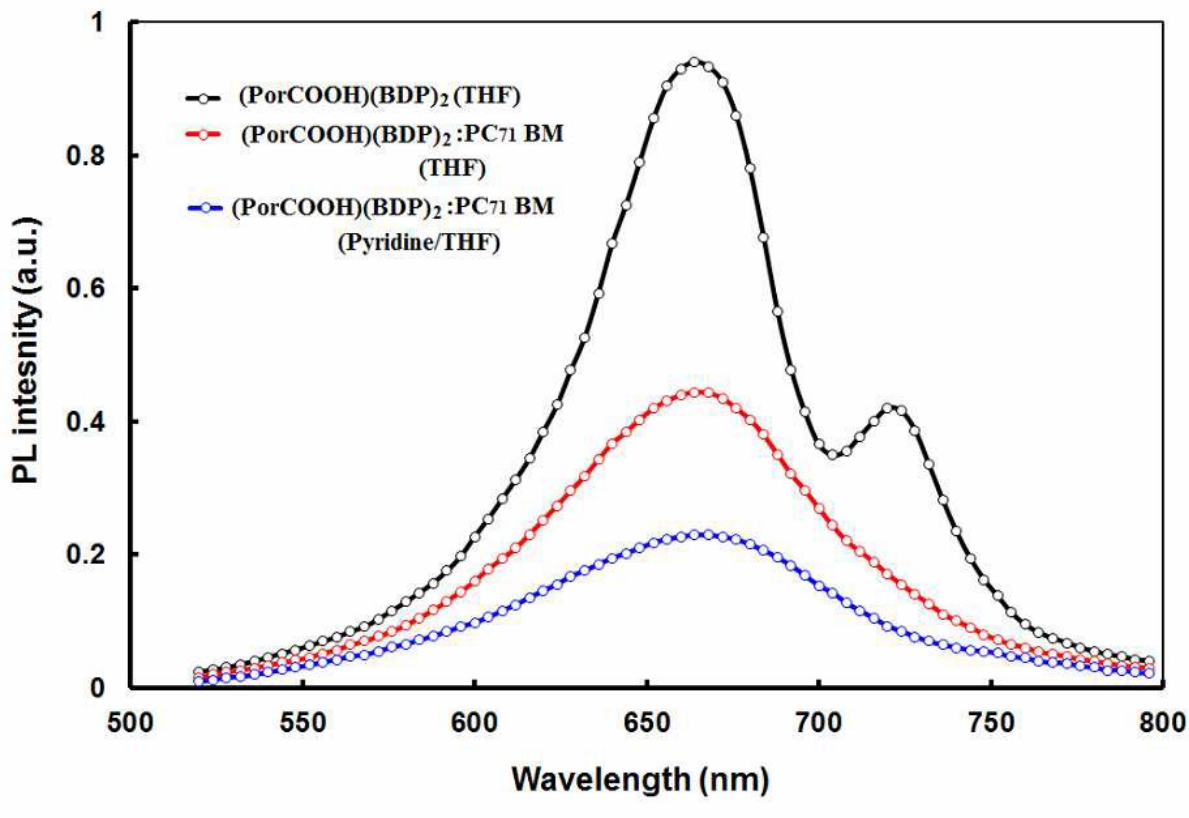

Figure 6: Photoluminenscence (PL) spectra of **(PorCOOH)(BDP)$_2$**, **(PorCOOH)(BDP)$_2$**: $PC_{71}BM$ (THF cast) and **(PorCOOH)(BDP)$_2$** :$PC_{71}BM$ (pyridine/THF cast) films.

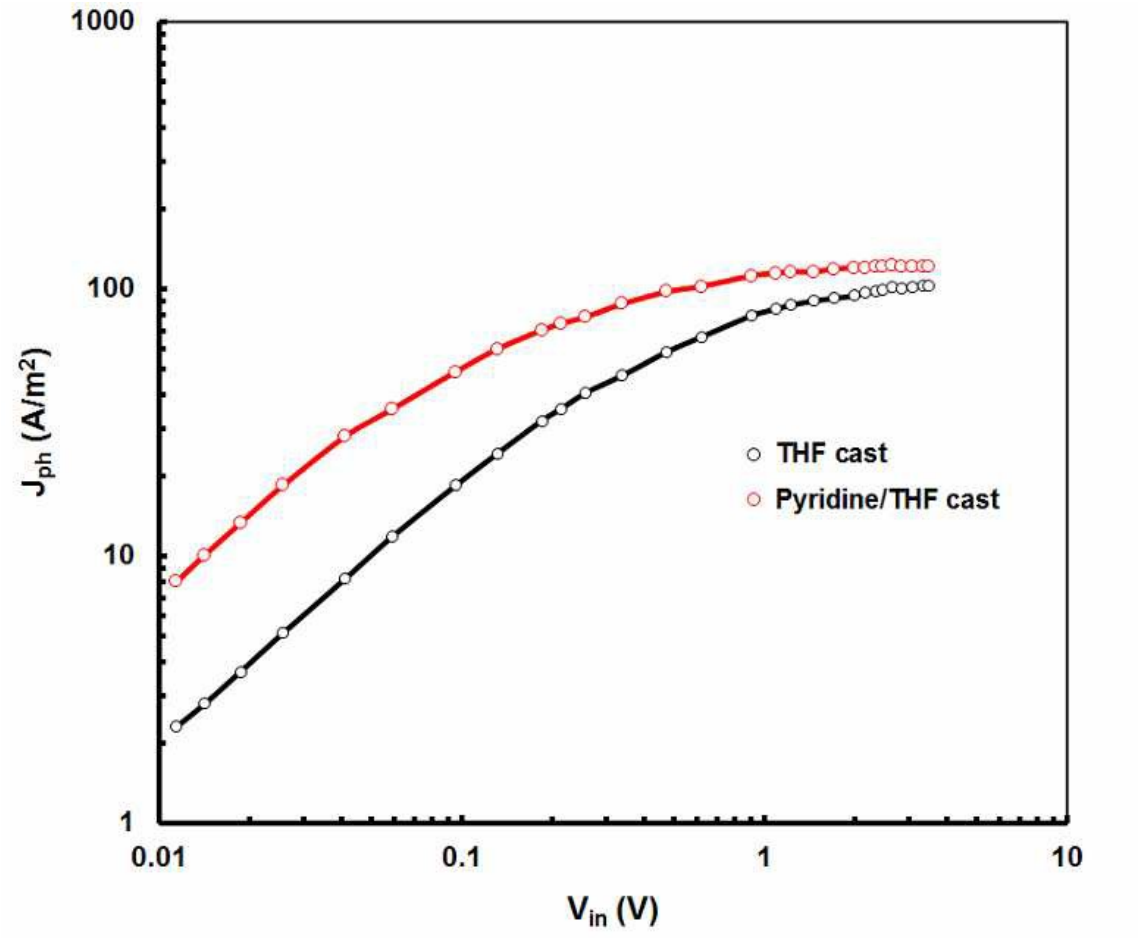

Figure 6: Variation of photocurrent density (J_{ph}) with the internal voltage (V_{in}) for devices processed with and without pyridine additives.

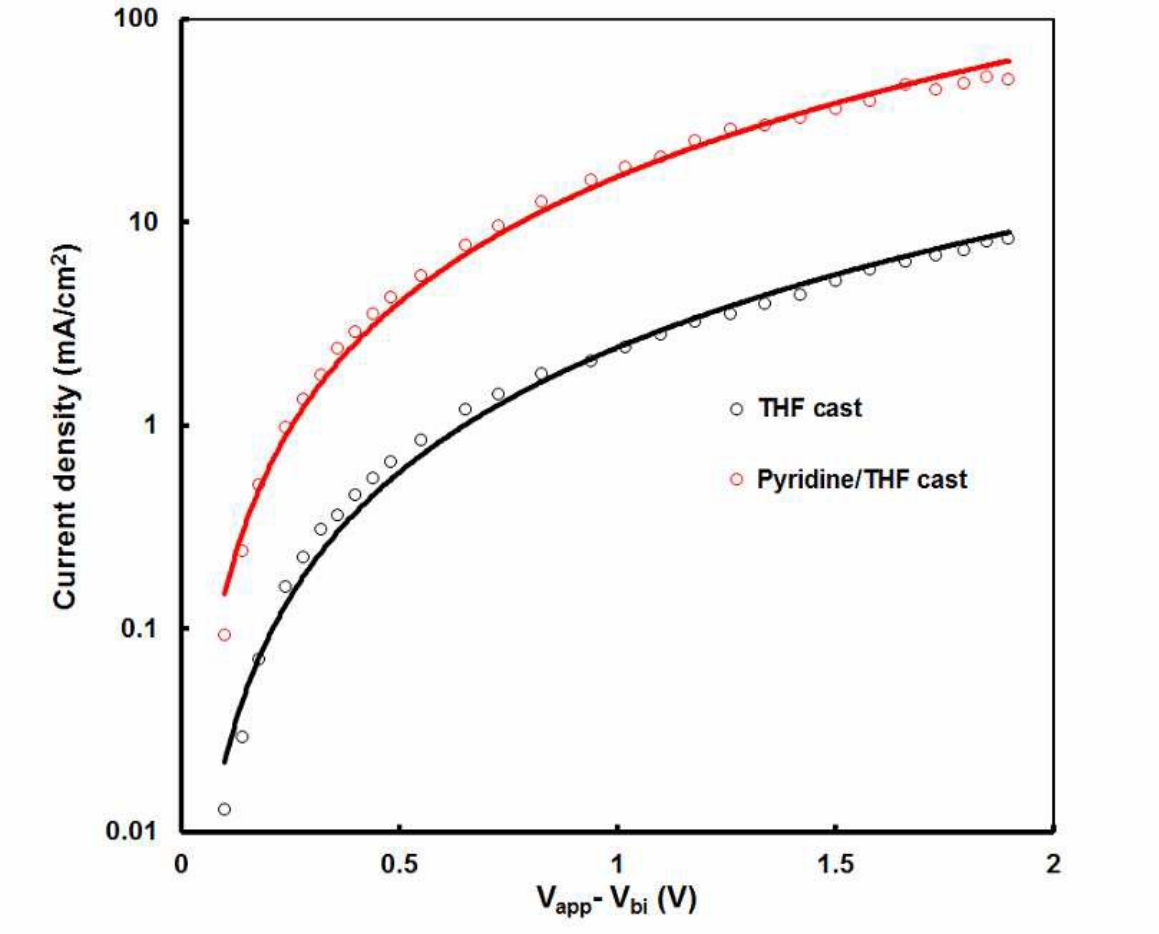

Figure 7: Dark current-voltage characteristics (J-V) of hole only devices based on the **(PorCOOH)(BDP)$_2$**:$PC_{71}BM$ active layer processed with THF and pyridine/THF solvents. The solid lines represent the fitting using SCLC model.

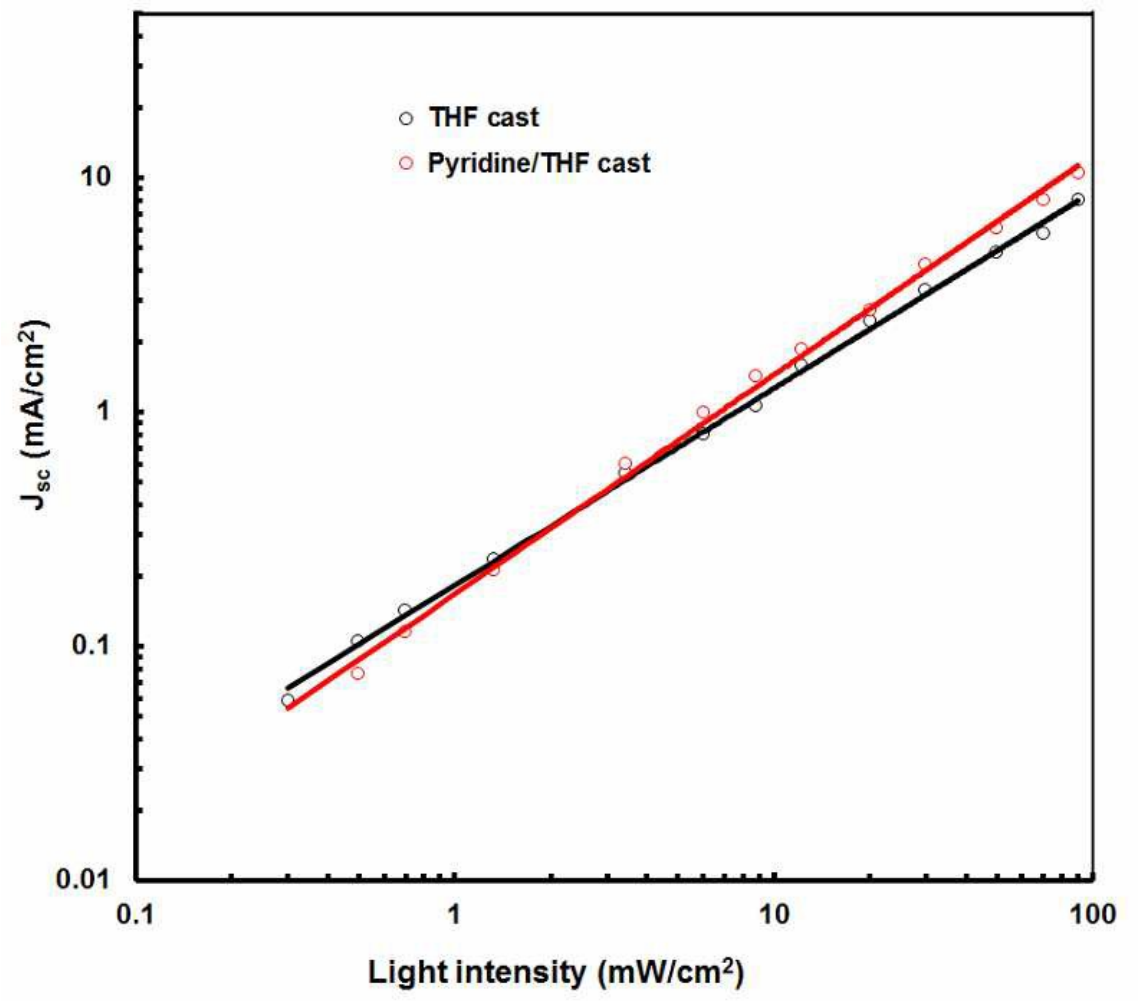

Figure 8: Variation of J_{sc} against light illumination intensity of organic solar cells based on the **(PorCOOH)(BDP)$_2$**:$PC_{71}BM$ active layer processed with THF and pyridine/THF solvents.